Polymer Chemistry

Accepted Manuscript

This is an *Accepted Manuscript*, which has been through the Royal Society of Chemistry peer review process and has been accepted for publication.

Accepted Manuscripts are published online shortly after acceptance, before technical editing, formatting and proof reading. Using this free service, authors can make their results available to the community, in citable form, before we publish the edited article. We will replace this *Accepted Manuscript* with the edited and formatted *Advance Article* as soon as it is available.

You can find more information about *Accepted Manuscripts* in the Information for Authors.

Please note that technical editing may introduce minor changes to the text and/or graphics, which may alter content. The journal's standard Terms & Conditions and the Ethical guidelines still apply. In no event shall the Royal Society of Chemistry be held responsible for any errors or omissions in this *Accepted Manuscript* or any consequences arising from the use of any information it contains.

ROYAL SOCIETY OF CHEMISTRY

www.rsc.org/polymers

Polymer Chemistry

ARTICLE

"DNA-Teflon" sequence-controlled polymers

Received 00th January 20xx,
Accepted 00th January 20xx

DOI: 10.1039/x0xx00000x

www.rsc.org/

Donatien de Rochambeau[a], Maciej Barłóg [b], T. G. W. Edwardson[a], Johans J Fakhoury[a], Robin S. Stein[a], Hassan S. Bazzi [b] and Hanadi F. Sleiman*[a].

Perfluorocarbons (PFC) are a promising class of molecules for medical applications: they are detectable through ^{19}F nuclear magnetic resonance (NMR) and they assemble separately from water or lipophilic phases, thus bringing unique supramolecular interactions into nanostructures. We report the ready insertion of PFCs into nucleic acids, as well as non-natural polymers in a sequence-defined fashion. This is achieved via an automated and efficient synthetic pathway using phosphoramidite chemistry. Modulating the PFC tail length of "DNA-Teflon" block copolymers resulted in micelles that are almost monodisperse, have low critical micelle concentration (CMC), are traceable by ^{19}F NMR and responsive to external stimuli. Strong fluorine-fluorine interactions in DNA duplexes allowed remarkable melting temperature increases and provided nuclease resistance. Finally, PFC insertion into siRNA was achieved, and the conjugates were efficient for gene silencing, outlining that these modifications are highly suitable for oligonucleotide therapeutics and bioimaging tools.

Introduction

Perfluorocarbons (PFC) present significant advantages for biological applications. They can be used as highly efficient oxygen carriers[1-3], and as labels for non-invasive imaging with medical resonance imaging (MRI)[4, 5]. Additionally, they can be tailored to improve efficiency of drug delivery[6, 7, 8] and affinity for cell membranes[9]. Oligonucleotides have emerged as a powerful class of potential therapeutics, because of their specificity, their ability to address undruggable targets and their inherent biocompatibility[10]. However, their clinical applications have been hampered by poor cellular penetration and stability to nucleases[11]. Perfluorocarbons can help overcome some of these factors. Indeed, it was shown that DNA[12] and PNA[13] modified with a single perfluorocarbon chain exhibit enhanced cellular penetration ability. Given their MRI imaging potential and the possibility to influence nucleic acid biological properties through the fluorous effect, the efficient synthesis of perfluorocarbon-DNA conjugates would of great interest towards the design of theranostic DNA structures.[14]

As supramolecular building blocks, perfluorocarbons tend to minimize interactions with other compounds by creating a separate phase from both hydrophilic and lipophilic phases; this phenomenon is termed the "fluorous effect"[15-17]. Introducing these units into DNA nanostructures can impart them with the fluorous effect as an orthogonal interaction to Watson-Crick base-pairing, thus increasing the structural range of DNA nanotechnology.

^{19}F MRI (magnetic resonance imaging) in the case of perfluoro-amphiphiles is known to be very challenging. To get high signal intensity, it requires a large number of fluorine atoms. However, aggregation of PFCs into an immobile phase can diminish or even completely suppress the signal[18-21]. The ability to tune the fluorine location and content in PFC containing polymers would allow fine adjustment of their assembly and optimization of MRI signals.

Sequence-defined polymer synthesis is a growing area that has recently attracted significant interest[22]. Current strategies rely on insertion of specific monomer units into polymer chains through chain-growth polymerization[23-25], or using short oligomers with defined sequences as monomers[26, 27]. For complete sequence control, the use of molecular machines[28], DNA-templated synthesis[29, 30] or sequential attachment of monomers[31-34] have been reported.

We report herein a versatile synthesis of sequence-controlled and monodisperse polymers containing

[a] Department of Chemistry
McGill University
801, Sherbrooke St. West, Montreal, QC, Canada. H3A 0B8.
E-mail: hanadi.sleiman@mcgill.ca
[b] Department of Chemistry
Texas A&M University at Qatar
P.O. Box 23874, Doha, Qatar.

Electronic Supplementary Information (ESI) available: detailed synthetic and purification protocols, additional characterization data, detailed procedures for ^{19}F NMR, thermal denaturation, nuclease resistance analyses and gene silencing experiments. See DOI: 10.1039/x0xx00000x

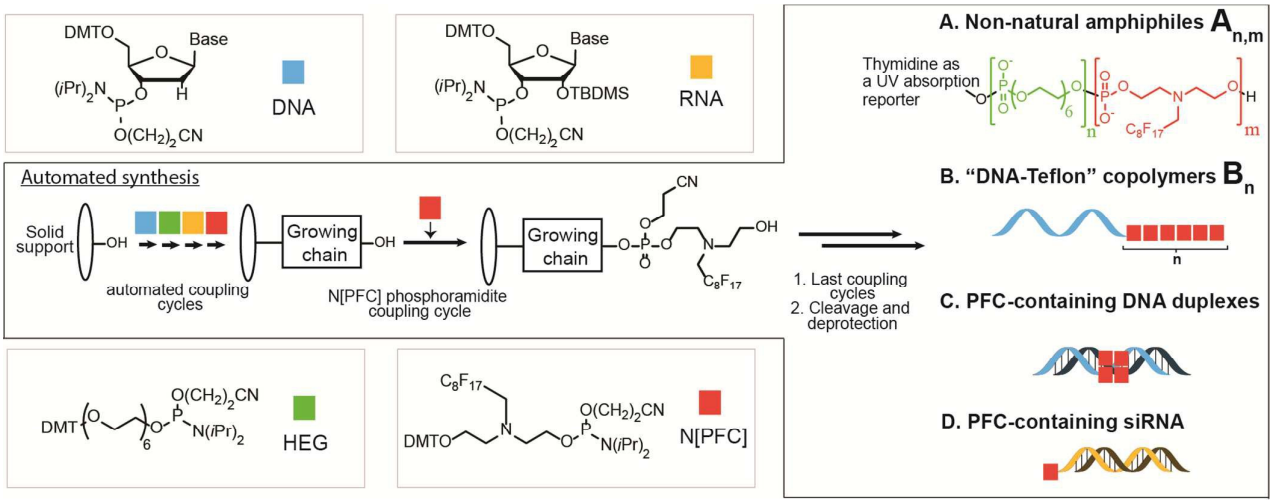

Figure 1. Synthesis of versatile sequence controlled oligomers with phosphoramidites grafted sequentially onto a growing chain attached to solid support. The automated synthetic cycle is described in details on Figure SF1.

perfluorocarbons, using automated phosphoramidite chemistry. This method yields non-natural polymers containing hydrophilic chains and PFCs in a precise sequence order. We then show the sequence-defined incorporation of PFC units into DNA strands. Due to the "fluorous effect", DNA-PFC precision polymers form micelles at low critical micelle concentrations (CMC) in aqueous media. The micelles have low polydispersity, their size can be switched by adding divalent cations in solution and, surprisingly, they can be readily detected through ^{19}F NMR. We find that the inclusion of two PFCs in a face-to-face arrangement within a DNA duplex results in remarkably high stabilization of DNA towards thermal denaturation[35] and significantly increased nuclease resistance. Finally, we synthesized siRNA (short interfering RNA)-PFC conjugates and showed their ability to effect gene silencing in mammalian cells.

Results and discussion

Synthesis of PFC sequence-controlled polymers

The synthesis of the phosphoramidite N[PFC] (Fig. 1 and Supplementary information, SI Scheme SS1) started with conversion of a commercial perfluorinated alcohol into its triflate, followed by heating with diethanolamine. Monoprotection with dimethoxytrityl chloride and conversion to the phosphoramidite[36, 37] gave N[PFC]. We first used theN[PFC] phosphoramidite to prepare non-natural copolymers with a hexaethylene glycol (HEG) hydrophilic block and a perfluorocarbon block. HEG phosphoramidite (commercially available) and N[PFC] were attached sequentially on a solid support using an automated DNA synthesizer (Fig. 1, polymers $\mathbf{A_{n,m}}$). In order to make our polymers UV detectable, we started the synthesis with a thymidine nucleotide on the hydrophilic extremity. Cleavage and deprotection were carried out using ammonium hydroxide at 60°C for 10 hours. Isolation of the final compounds was performed using RP-HPLC (reverse phase high performance liquid chromatography) and purity was checked by LCMS (liquid chromatography-mass spectroscopy, Figure SF3). Yields were measured with RP-HPLC (Table ST1, Figure SF2). The synthetic and purification methods are facile and extremely efficient, and lead to amphiphilic monodisperse polyphosphates with precise numbers and sequences of HEG and PFC units, and masses up to 5 kDa ($\mathbf{A_{8,4}}$) in very good yields.

We then incorporated N[PFC] on the 5'-end of a DNA strand on the automated DNA synthesizer (polymers $\mathbf{B_n}$). Interestingly, we could successfully attach up to ten N[PFC] units on a 19-mer (equivalent to 6 kDa polymer). Cleavage from the solid support, isolation, determination of yield and purity were carried out as above (Table 1, Fig. 2). A single N[PFC] addition showed excellent coupling yields (>95%) and grafting several N[PFC] was very efficient. This is noteworthy, considering that the attachment of highly hydrophobic units to DNA is often challenging[12, 38, 39]. 1 to 3 N[PFC] units were also incorporated at internal positions of two complementary DNA strand (Fig. SF5, Table ST3).

It is important to note here that the N[PFC] unit contains a tertiary amine moiety. We were thus initially surprised that it could be incorporated so readily in phosphoramidite-based synthesis and coupling. Interestingly, if the C_8F_{17} moiety in N[PFC] is replaced by a $C_{15}H_{31}$ chain on the nitrogen, very poor

Table 1. Yields and ESI-MS characterization of different DNA-"Teflon" hybrids $\mathbf{B_n}$.

Number of PFC units (n)	HPLC yields[a] [%]	Calculated exact mass [g mol^{-1}]	Found exact mass [g mol^{-1}]
1	95	6364.01	6364.00
2	86	6963.02	6963.00
4	76	8161.05	8161.00
6	73	9362.89 (MW[b])	9362.13 (MW)
10	74	11759.61 (MW)	11758.95 (MW)

[a] Calculated through the integration of the peak associated to the expected product (260 nm detection). [b] MW stands for molecular weight.

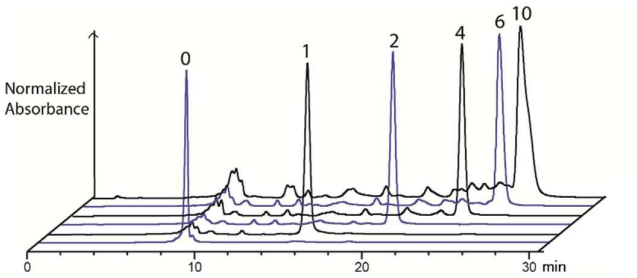

Figure 2. Reverse-phase (RP) HPLC traces (UV detection, 260 nm) from crude mixtures. Numbers on the peaks are the number (n) of N[PFC] attached on the 19-mer.

yields and further degradation of the modified strand are observed. We suggest that in the $C_{15}H_{31}$ case, the nitrogen lone pair is nucleophilic enough to intramolecularly react with the electrophilic phosphoramidite, as well as the phosphate on the final DNA strand, via 5-membered ring transition states (Figure SF17). On the other hand, N[PFC]-modified DNA strands are obtained in high yields and can be stored for several weeks in a fridge in solution with minor degradation. This difference is likely due to the strong inductive effect of the PFC, which decreases the nitrogen nucleophilicity.

DNA-"Teflon" polymers self-assembly studies

Dynamic light scattering (DLS) indicates self-assembly of strands **B_2**, **B_4**, **B_5** and **B_{10}** (Fig. SF13, Table ST4) in water at small concentrations (10 µM). Strikingly, the nanostructures are almost monodisperse (polydispersity index, PDI<16%, Fig. 3b,c). Figure 3a shows atomic force microscopy (AFM) images of the DNA conjugate with 5 N[PFC] units. Spherical structures of uniform sizes and average radii (R_{AFM}) of 9.7 nm were observed, consistent with the DLS analysis (additional images in figures SF10, SF11). Because of their monodisperse nature and unlike regular polymers, **B_4**, **B_5** and **B_{10}** conjugates likely assemble into spherical micelles of narrow size distribution, with a perfluorocarbon core and a DNA corona. **B_n** conjugates contain perfluorocarbon chains punctuated by phosphate groups. Interestingly, we found that the addition of magnesium ions significantly alters their assembly[40]. While **B_2** does not aggregate in pure water, addition of Mg^{2+} triggers assembly (SI-IV.c). Upon Mg^{2+} addition, micelles from DNA strands with 4 or 5 PFC units undergo a significant radius decrease within one minute (R_{DLS} ~8 nm to 6 nm, Table ST4). The Mg^{2+} cations likely coordinate the negatively charged phosphate groups between the PFC units and on the DNA strands, thus decreasing their repulsive electrostatic interactions (Fig. 3c). It is noteworthy that the precise control over the perfluorocarbon block size of our constructs allows modulation of their assembly properties. DLS allowed us to determine that the critical micellar concentration (CMC) of the conjugates is small (below 10 µM). In addition, gel electrophoresis results suggest that micelles still form at 1 µM (fig. SF9). Due to the DNA-Teflon micelles' narrow polydispersity and low CMC, they are highly likely to be useful for drug delivery applications of fluorine containing drugs.

^{19}F NMR detection of DNA-"Teflon" micelles

Given their unique architecture, we examined the ^{19}F NMR properties of our conjugates. Spectra were acquired of (i) N[PFC] diol (**2**, see Fig. SS1), (ii) **B_1**, (iii) **B_4** micelles, and (iv) **B_{10}** micelles. Surprisingly, even in the core of micelle structures, N[PFC] units were detected through their CF_3 moiety at low strand concentration (46 µM). ^{19}F spin-lattice relaxation (T_1) and spin-spin relaxation (T_2) were measured at 11.7 T (SI-IV.d). As expected, self-assembly led to a decrease of T_2 from 180 ms for **B_1** to 7 ms for **B_4** and 2.0 ms for **B_{10}**. However, these values are still acceptable for potential MRI applications compared to those described elsewhere[21]. At the same time, we observed a decrease of T_1 with the number of N[PFC] units: T_1=740 ms, 160 ms and 150 ms respectively

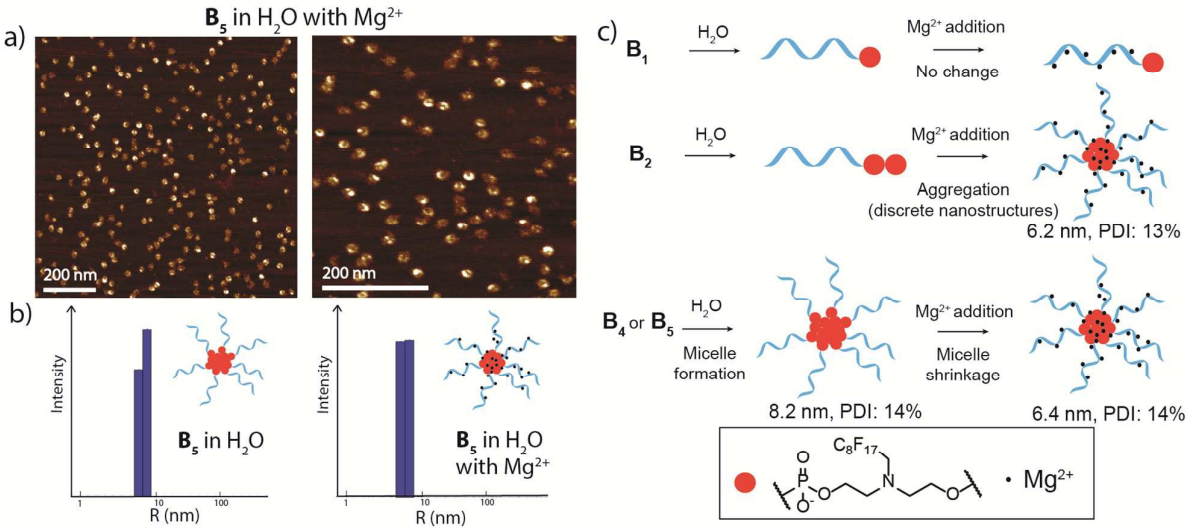

Figure 3. a) Dry AFM images. **B_5** deposited on mica. Scale bar: 200 nm. We believe the features observed by AFM possibly arise from partial collapse of the DNA strands on the mica surface, and protrusion of the perfluoro- block above the micelle due to repulsion from the mica. b) Hydrodynamic radius distribution of **B_5** in H_2O (left) and B_5 in H_2O with Mg^{2+} (7.6 mM) (right) obtained by DLS. The histogram illustrates the narrow polydispersity of the micelles. c) Effect of sequence-control and Mg2+ addition for DNA-Teflon copolymers assembly. Micelles radii and PDI obtained by DLS are reported under the micelles

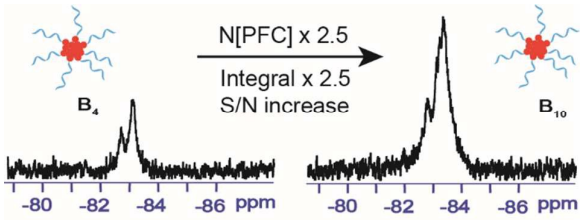

Figure 4. ^{19}F NMR spectra of $\mathbf{B_4}$ (left) and $\mathbf{B_{10}}$ (right) in D_2O. Acquisition conditions detailed in SI-IV.d (S/N=signal to noise ratio).

for $\mathbf{B_1}$, $\mathbf{B_4}$ and $\mathbf{B_{10}}$. The short T_1 of the micelle samples allows for the possibility of acquiring many scans in short time periods, therefore increasing the signal intensity.

We were interested in specifically comparing the NMR signal of micelles with a large number of N[PFC] per strand ($\mathbf{B_{10}}$) to the sensitivity of $\mathbf{B_4}$. A higher signal-to-noise ratio (*S/N*) was observed for $\mathbf{B_{10}}$ (24.3) than for $\mathbf{B_4}$ (14.4) after fifteen minutes acquisition, when both samples are analyzed under identical conditions (Fig. 4). Moreover, due to shorter relaxation times for $\mathbf{B_{10}}$, sensitivity was enhanced even more (*S/N*=32.6). Modulating the number of N[PFC] units through sequence-control and having a polyphosphate backbone are particularly promising approaches to control sensitivity for MRI applications.

Since the low fluorine background from biological samples allows for ^{19}F MRI quantification[41], we also determined micelle concentrations using quantitative ^{19}F NMR. We measured the concentrations of NMR samples (ii), (iii), and (iv) with regards to an external reference made with molecule **2**. Results were close to the concentrations obtained by UV absorption even in the case of micelles (±10%, Table ST6) showing that self-assembly does not prevent the retrieval of most of the CF_3 signal. These results highlight the potential of the N[PFC] DNA modifications for bio-imaging with possible micelle quantification.

"Fluorous" effect and nuclease resistance in PFC-containing DNA duplexes

DNA duplex stability and nuclease resistance are important requirements for the *in vivo* applications of this molecule. We assessed the effect of N[PFC] insertions on DNA thermal denaturation. With a single insertion on each strand of complementary 19mers, such that they face each other in the duplex ($\mathbf{C_2}$, fig. 5a), a slight increase of ~0.5°C in the thermal denaturation temperature (T_M) is observable. On the other hand, when two adjacent N[PFC] units are incorporated within each strand, a dramatic T_M increase of about 8°C is detected ($\mathbf{C_3}$). This stabilization is similar to that of the replacement of two nucleotides with locked nucleic acid (LNA) nucleotides, considering the length of our DNA strand[35]. If the two modifications on each strand are not adjacent ($\mathbf{C_4}$), the T_M increase is much less pronounced. The PFC chains thus likely associate into a "fluorous" environment, avoiding unfavorable interactions in water, and leading to significant stabilization for DNA duplexes. When residing on the duplex end, a single modification on each strand ($\mathbf{C_5}$) increases the T_M by 2 °C.

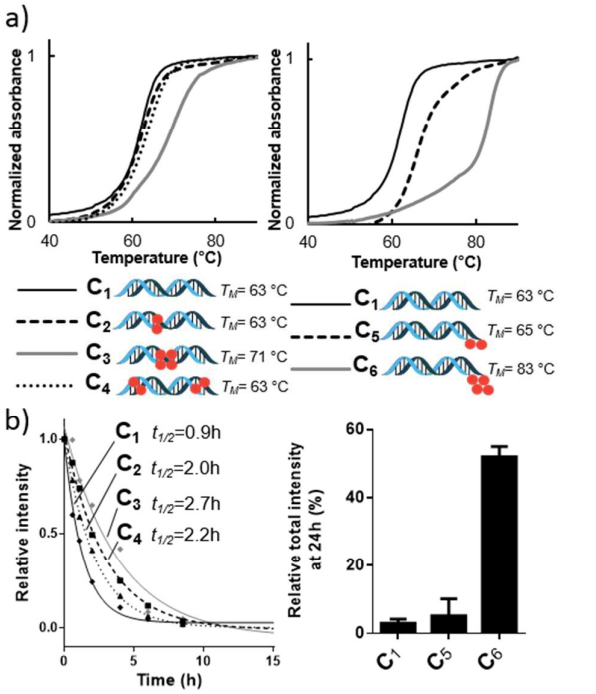

Figure 5. a) Representative melting temperature curves of PFC-containing DNA 19mer duplexes. Red spheres represent the N[PFC] modification. Left: internal modifications. Right: external modifications. See table ST7 for exact sequences of duplexes $\mathbf{C_n}$. Experimental details in SI-V.b. b). Nuclease resistance properties of modified DNA duplexes. Left: Average of PFC-containing DNA duplexes degradation curves. Right: percentage of DNA detected on gel after 24h relatively to the amount detected initially. Goodness of fits and discussion are presented in the supplementary material (SI-V.c).

Interestingly, a remarkable increase of 20°C is obtained with two modifications on each strand end ($\mathbf{C_6}$). (Fig. 5a, some aggregation detected Fig. SF12, SF13). The N[PFC] insertions and the fluorous effect provide a simple method to modulate DNA stability across a range of melting temperatures, and will be valuable for building complex structures from DNA.

Having observed the stabilization they impart on DNA hybridization, we examined the influence of N[PFC] insertions on nuclease resistance. For this, we exposed an unmodified 19mer duplex and DNA-PFC conjugates to foetal bovine serum (FBS) in Dubelcco modified Eagle's minimal essential medium (DMEM) at 37°C. Aliquots were collected at specific time-points and the nucleases were quenched at low temperature as previously reported[42]. DNA in each aliquot was analyzed through quantitative gel electrophoretic mobility assays to determine the half-life of the different strands in FBS. The $\mathbf{C_2}$ duplex with a single insertion in each strand showed better nuclease resistance than unmodified DNA; interestingly, two adjacent modifications even enhanced DNA half-life by a factor of 3 (Fig. 5b). Due to the incompatibility of a one phase decay model for $\mathbf{C_5}$ and $\mathbf{C_6}$ (see SI-V.c), we chose to quantify the total detectable amount of oligonucleotides at each time-point. With two modifications on the end of each DNA strand, $\mathbf{C_6}$ shows impressive nuclease resistance properties, as ~50% of the initial detected DNA was still present after 24h incubation, while only 3% of C_1 was detected after 24h. Thus, in addition

to the capacity for bioimaging by ^{19}F NMR, the perfluorocarbon modifications very significantly increase DNA stability and nuclease resistance.

PFC-containing siRNA silencing properties

The PFC conjugation to DNA is highly advantageous for biological applications. We were interested to examine if PFC could also be introduced into small interfering RNA strands (siRNA) and whether these constructs would still be therapeutically active. For this experiment, we chose siRNA for Apolipoprotein B[43] and modified the 3'-end of the sense strand with a single N[PFC] unit. Yields were close to those usually obtained for unmodified RNA synthesis and LCMS characterization verified the conjugate's identity (Figure SF5). We transfected unmodified siRNA and PFC-modified siRNA into HepG2 cells (liver carcinoma) and incubated the cells for 24 hours. Total RNA was then collected from the cells and reverse transcribed the RNA to cDNA, followed by quantification of ApoB mRNA (messenger RNA) using qRT-PCR (quantitative real-time polymerase reaction). We observed that the modified siRNA is able to cause a 50% reduction in ApoB mRNA levels, and retains its activity as compared to unmodified siRNA (Fig. 6). Thus, PFC chains can be incorporated into therapeutic oligonucleotides, and do not interfere with their potency. With the ability to control the sequence, position and length of PFC-insertions, we anticipate being able to further optimize this silencing effect; importantly, we expect that the significant DNA stability, nuclease resistance, nanoscale micelle size and altered cellular penetration[12,13] provided by the PFC units to significantly enhance the in vivo delivery of nucleic acid therapeutics.

Conclusions

In conclusion, we highlight the efficiency of automated phosphoramidite chemistry to generate sequence-controlled amphiphiles with perfluorocarbons units. Monodisperse polymers with hydrophilic, fluorophilic and DNA blocks were synthesized. Precise control of the number and location of each of the monomers on the polymer chain was possible and gave rise to different properties in each case. PFC chains can significantly increase the thermal stability (by up to 20°C) and nuclease resistance of DNA strands, and they result in the self-assembly of monodisperse micellar nanoparticles. Interestingly, even with this self-assembly, the micelles are readily observable by ^{19}F NMR. Perfluorocarbons were also introduced into siRNA, and the conjugate remained potent as a gene silencing agent. A full study of toxicity and *in vivo* bioaccumulation[44] has yet to be performed, but PFCs are inert and usually considered as safe[45]. DNA- and RNA-perfluorocarbon conjugates are highly likely to be valuable for therapeutic and theranostic applications, given their stability, monodisperse, nanometer sized micelle formation, ability for gene silencing, and their potential for detection *in vivo* by magnetic resonance imaging.

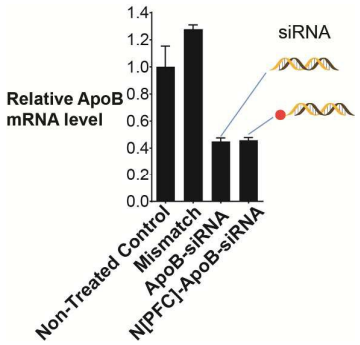

Figure 6. Gene silencing assay results. Gene expression is reduced by 50% in cells transfected by modified and unmodified siRNA. Mismatch is a negative control as its sequence should not induce gene silencing.

Acknowledgements

The authors thank the National Sciences and Engineering Research Council (NSERC) and the Qatar National Research Fund (QNRF) for support (project number NPRP 5 - 1505 - 1 – 250). D. de Rochambeau thanks Canadian Institutes of Health Research (CIHR) for a Drug Development Training Program (DDTP) scholarship and NSERC for a CREATE training program in Bionanomachines (CTPB) scholarship. We thank Dr. Alexander Wahba for his help with MS characterization.

Notes and references

1. L. C. Clark and F. Gollan, *Science*, 1966, **152**, 1755-1756.
2. D. R. Spahn, *Critical care (London, England)*, 1999, **3**, R93-97.
3. C. I. Castro and J. C. Briceno, *Artificial organs*, 2010, **34**, 622-634.
4. J. Chen, G. M. Lanza and S. A. Wickline, *Wiley Interdiscip. Rev.: Nanomed. Nanobiotechnol.*, 2010, **2**, 431-440.
5. J. Ruiz-Cabello, B. P. Barnett, P. A. Bottomley and J. W. M. Bulte, *NMR Biomed.*, 2011, **24**, 114-129.
6. P. Vierling, C. Santaella and J. Greiner, *J. Fluorine Chem.*, 2001, **107**, 337-354.
7. M. Wang, H. Liu, L. Li and Y. Cheng, *Nat. Commun.*, 2014, **5**, 3053.
8. H. Wang, Y. Wang, Y. Wang, J. Hu, T. Li, H. Liu, Q. Zhang and Y. Cheng, *Angew. Chem. Int. Ed. Engl.*, 2015, **54**, 11647-11651.
9. M. C. Z. Kasuya, S. Nakano, R. Katayama and K. Hatanaka, *J. Fluorine Chem.*, 2011, **132**, 202-206.
10. N. Dias and C. A. Stein, *Molecular Cancer Therapeutics*, 2002, **1**, 347-355.
11. R. L. Juliano, X. Ming, K. Carver and B. Laing, *Nucleic Acid Therapeutics*, 2014, **24**, 101-113.
12. G. Godeau, H. Arnion, C. Brun, C. Staedel and P. Barthélémy, *MedChemComm*, 2010, **1**, 76.
13. S. Ellipilli, R. Vasudeva Murthy and K. N. Ganesh, *Chem. Commun.*, 2016, **52**, 521-524.
14. H. Pei, X. Zuo, D. Zhu, Q. Huang and C. Fan, *Acc. Chem. Res.*, 2014, **47**, 550-559.
15. M. Cametti, B. Crousse, P. Metrangolo, R. Milani and G. Resnati, *Chem. Soc. Rev.*, 2012, **41**, 31-42.

16. R. Berger, G. Resnati, P. Metrangolo, E. Weber and J. Hulliger, *Chem. Soc. Rev.*, 2011, **40**, 3496-3508.
17. D. A. Tomalia, *Nature materials*, 2003, **2**, 711-712.
18. M. Oishi, S. Sumitani and Y. Nagasaki, *Bioconjugate Chem.*, 2007, **18**, 1379-1382.
19. Y. Takaoka, T. Sakamoto, S. Tsukiji, M. Narazaki, T. Matsuda, H. Tochio, M. Shirakawa and I. Hamachi, *Nat. Chem.*, 2009, **1**, 557-561.
20. H. Wang, K. R. Raghupathi, J. Zhuang and S. Thayumanavan, *ACS Macro Lett*, 2015, **4**, 422-425.
21. S. Bo, C. Song, Y. Li, W. Yu, S. Chen, X. Zhou, Z. Yang, X. Zheng and Z.-X. Jiang, *J. Org. Chem*, 2015, **80**, 6360-6366.
22. J.-F. Lutz, M. Ouchi, D. R. Liu and M. Sawamoto, *Science*, 2013, **341**, 1238149.
23. S. Pfeifer and J.-F. Lutz, *J. Am. Chem. Soc.*, 2007, **129**, 9542-9543.
24. M. Zamfir and J.-F. Lutz, *Nat. Commun.*, 2012, **3**, 1138.
25. T. Terashima, T. Mes, T. F. A. De Greef, M. A. J. Gillissen, P. Besenius, A. R. A. Palmans and E. W. Meijer, *J. Am. Chem. Soc.*, 2011, **133**, 4742-4745.
26. Z.-L. Li, L. Li, X.-X. Deng, L.-J. Zhang, B.-T. Dong, F.-S. Du and Z.-C. Li, *Macromolecules*, 2012, **45**, 4590-4598.
27. K. Satoh, S. Ozawa, M. Mizutani, K. Nagai and M. Kamigaito, *Nat. Commun.*, 2010, **1**, 6.
28. B. Lewandowski, G. De Bo, J. W. Ward, M. Papmeyer, S. Kuschel, M. J. Aldegunde, P. M. E. Gramlich, D. Heckmann, S. M. Goldup, D. M. D'Souza, A. E. Fernandes and D. a. Leigh, *Science*, 2013, **339**, 189-193.
29. P. J. Milnes, M. L. McKee, J. Bath, L. Song, E. Stulz, A. J. Turberfield and R. K. O'Reilly, *Chem. Commun.*, 2012, **48**, 5614-5616.
30. J. Niu, R. Hili and D. R. Liu, *Nat. Chem.*, 2013, **5**, 282-292.
31. R. N. Zuckermann, J. M. Kerr, S. B. H. Kent and W. H. Moos, *J. Am. Chem. Soc.*, 1992, **114**, 10646-10647.
32. J. Sun and R. N. Zuckermann, *{ACS} Nano*, 2013, **7**, 4715-4732.
33. A. Al Ouahabi, L. Charles and J.-F. Lutz, *J. Am. Chem. Soc.*, 2015, **137**, 5629-5635.
34. T. G. W. Edwardson, K. M. M. Carneiro, C. J. Serpell and H. F. Sleiman, *Angew. Chem. Int. Ed.*, 2014, **53**, 4567-4571.
35. D. A. Braasch and D. R. Corey, *Chemistry & Biology*, 2001, **8**, 1-7.
36. S. L. Beaucage, *Methods in molecular biology (Clifton, N.J.)*, 1993, **20**, 33-61.
37. Y. Dong, D. Liu and Z. Yang, *Methods*, 2014, **67**, 116-122.
38. D. Kedracki, I. Safir, N. Gour, K. X. Ngo and C. Vebert-Nardin, *Bio-synthetic Polymer Conjugates*. H. Schlaad, Springer Berlin Heidelberg**:** 115-149.
39. M. Kwak and A. Herrmann, *Chem. Soc. Rev.*, 2011, **40**, 5745-5755.
40. M.-P. Chien, A. M. Rush, M. P. Thompson and N. C. Gianneschi, *Angew. Chem. Int. Ed.*, 2010, **49**, 5076-5080.
41. E. T. Ahrens and J. Zhong, *NMR Biomed.*, 2013, **26**, 860-871.
42. J. W. Conway, C. K. McLaughlin, K. J. Castor and H. Sleiman, *Chem. Commun.*, 2013, **49**, 1172-1174.
43. J. Soutschek, A. Akinc, B. Bramlage, K. Charisse, R. Constien, M. Donoghue, S. Elbashir, A. Geick, P. Hadwiger, J. Harborth, M. John, V. Kesavan, G. Lavine, R. K. Pandey, T. Racie, K. G. Rajeev, I. Röhl, I. Toudjarska, G. Wang, S. Wuschko, D. Bumcrot, V. Koteliansky, S. Limmer, M. Manoharan and H.-P. Vornlocher, *Nature*, 2004, **432**, 173-178.
44. C. Lau, J. L. Butenhoff and J. M. Rogers, *Toxicol. Appl. Pharmacol.*, 2004, **198**, 231-241.
45. K. Hintzer, T. Zipplies, D. P. Carlson and W. Schmiegel, in *Ullmann's Encyclopedia of Industrial Chemistry*, Wiley-VCH Verlag GmbH & Co. KGaA, 2000, DOI: 10.1002/14356007.a11_393.pub2.

Efficient automated synthesis of sequence-controlled “DNA-Teflon” polymers with potential drug delivery and bioimaging applications.